

X-ray single phase LSGM at 1350 °C

Cinar Oncel*, Berkem Ozkaya¹, Mehmet Ali Gulgun

Sabanci University, Faculty of Engineering and Natural Sciences, Tuzla, Istanbul, Turkey

Available online 3 July 2006

Abstract

Synthesis of X-ray-phase-pure ($\text{La}_{1-x}\text{Sr}_x\text{Ga}_{1-y}\text{Mg}_y\text{O}_{3-\delta}$, LSGM, where $x=0.1$, $y=0.15$ and 0.17) powders were achieved at temperatures as low as 1350 °C via organic precursor method using tartaric acid as the carrier material. LSGM materials were characterized for their phase purity, crystallization and electrical properties. Pellets sintered at 1350 °C for 6 h were single phase and dense (>99%). Electron microscopy analysis of X-ray single-phase pellets revealed MgO precipitates with sizes ranging from 50–300 nm. Phase formation and distribution in this complicated multi-cation-oxide system as a function of temperature were reported and discussed. Amorphous LSGM first crystallizes at 625 °C. However, elimination of undesired phases require higher temperatures. Impedance measurements as a function of temperature up to 545 °C revealed that the X-ray phase pure pellets may have extrapolated ionic conductivity values as high as 0.14–0.16 S/cm at 800 °C. Possible implications of limited MgO solubility on the ionic conductivity are presented.

© 2006 Elsevier Ltd. All rights reserved.

Keywords: LSGM; Ionic conductivity; Solubility; MgO; Crystallization

1. Introduction

Sr- and Mg-doped LaGaO_3 perovskites have been studied extensively because of their high ionic conductivity at relatively low temperatures compared to the current electrolyte, yttria stabilized zirconia (YSZ), for solid oxide fuel cells (SOFC).^{1,2} YSZ electrolyte can provide the required ionic conductivity (0.1 S/cm) for effective SOFC operation only at temperatures in excess of 1000 °C. In comparison, LSGM electrolyte was reported to reach same or higher conductivity values around 800 °C (Table 1). Until now one of the best ionic conductivity values (0.17 S/cm at 800 °C) were achieved with the $\text{La}_{0.8}\text{Sr}_{0.2}\text{Ga}_{0.83}\text{Mg}_{0.17}\text{O}_{3-\delta}$ composition of Sr and Mg-doped LaGaO_3 (LSGM).⁵ The high ionic conductivity of the mixed oxide is ultimately linked to the amount of oxygen vacancies in the material. Additional oxygen vacancies are due to the Sr^{2+} and Mg^{2+} impurities replacing La^{3+} and Ga^{3+} in their lattice sites, respectively. It is thus desired to increase the Sr and Mg concentration without destroying the homogeneity of the system. Phase purity is critical to optimize ionic conductivity of LSGM.

Undesired phases act as obstacles for oxygen ion conduction through the material.

Method of synthesis for multi-cation-oxides is important in terms of the final properties of the oxide.^{6,7} Solid state reaction (SSR) method is the preferred choice of processing in a laboratory environment due to its simplicity. However, SSR has problems with the homogeneity of the oxide/carbonate mixture,^{8,9} and relatively high calcination temperatures.¹⁰ Organic precursor method eliminates such problems by starting with dissolved salts of the constituents of the final product mixed homogeneously in an aqueous media.¹¹ Complexing and/or chelating of the cations by the proper organic carrier material tend to decrease calcination temperature to reach the desired product.¹² Therefore, organic precursor method seems to be the most suitable method for synthesizing single phase multi-cation oxide powders at low temperatures. Using this method, the lowest theoretical temperature to produce the desired powders would be the crystallization temperature of the mixed oxide phase. Until today, LSGM was observed to crystallize at temperatures as low as 700 °C.¹³

Another important aspect regarding the SOFC electrolytes besides their high ionic conductivity is their gas-tightness which depends on the porosity level of the solid body. It has been reported that densification of LSGM powder compacts requires high temperatures (>1400 °C).^{14,15} However, LSGM was reported to lose gallium from its composition at

* Corresponding author at: Sabanci University, FENS, 34956, Tuzla, Istanbul, Turkey. Tel.: +905334587763; fax: +902164839550.

E-mail address: cinaroncel@su.sabanciuniv.edu (C. Oncel).

¹ Present address: University of Ulm, Albert Einstein Allee 39, D89081, Ulm, Germany.

Table 1
Ionic conductivities of YSZ and LSGM for 600 °C, 800 °C, and 1000 °C

Electrolyte	600 °C	800 °C	1000 °C
YSZ ³	0.003 S/cm	0.03 S/cm	0.1 S/cm
LSGM ^{3,4}	0.02 S/cm	0.12–0.17 S/cm	0.25 S/cm

temperatures in excess of 1400 °C, especially under reducing atmospheres.¹⁶ Thus, sintering at temperatures >1400 °C is not desired.¹⁷ Ga loss constitutes a severe problem in terms of the ionic conductivity of the material. As Ga leaves the system, the composition of the electrolyte changes and undesired phases appear which suppress total ionic conductivity of the material.¹⁶ Small variations in the composition result in large ionic conductivity changes.¹⁸ Thus, the control of composition plays an important role in the final properties of the electrolyte. Especially, solubility limit of the dopants, i.e., magnesium and strontium ions, in the lanthanum gallate matrix need to be determined to strike the optimum composition of the oxide.

In this study, crystallization temperature, low temperature synthesis, sintering, and ionic conductivity of LSGM material were studied. Solubility of magnesium and strontium in LaGaO₃ matrix were discussed.

2. Experimental

Chemical synthesis of the four-cation oxide material, LSGM (La_{0.9}Sr_{0.1}Ga_{1-x}Mg_xO_{3-δ}; $x = 0.15$ and 0.17) was investigated. For the synthesis, desired amounts of cation salts were measured and dissolved in distilled water to obtain exact stoichiometry in solution. The amount of carrier material was determined to obtain 1:1 ratio of cation to tartaric acid molecule in the aqueous solution. Thus, for example, for one mole of total cations, one mole organic carrier molecule (TA) was added to the solution.

Cation sources were nitrate salts selected for their high solubility in cold water (i.e., lanthanum nitrate hexahydrate (La(NO₃)₃·6H₂O, >99%, Sigma–Aldrich Chemie GmbH, Taufkirchen, Germany), gallium nitrate nanohydrate (Ga(NO₃)₃·9H₂O, 99.9%, ChemPur Feinchemikalien und Forschungsbedarf GmbH, Karlsruhe, Germany), strontium nitrate (Sr(NO₃)₂, >99%, Sigma–Aldrich Chemie GmbH, Taufkirchen, Germany), and magnesium nitrate hexahydrate (Mg(NO₃)₂·6H₂O, >99%, Merck KgaA, Darmstadt, Germany) for lanthanum, gallium, strontium and magnesium, respectively). Tartaric acid (C₄H₆O₂, 99.7%, Sigma–Aldrich Chemie GmbH, Taufkirchen, Germany) was the organic material of choice used as “carriers” for the cations.^{19,20}

Solution with the organic carrier and the cation salts was mixed with a magnetic stirrer and heated up to ~300 °C on a hot plate to evaporate the solvents and to obtain a crisp powder. The powders were calcined at 1150 °C in a box furnace with 10 °C/min heating rate in air. After reaching the final temperature the furnace was turned off immediately and the powders were allowed to cool in the furnace. After calcination, crystal structure and phase distribution of the powders were studied with an X-ray powder diffractometer (Bruker AXS-D8, Karlsruhe, Germany). The measurements were performed in the 2θ

range of 20°–50° at 40 kV and 40 mA, using CuK_α radiation. In all measurements, the step size was 0.03°, and data collection period was 2 s in each step. K_{α2} peaks were suppressed in the X-ray diffraction measurements by a monochromator. Calculation of the percentages of each phase on X-ray diffraction data was described elsewhere.²⁰ For phase identification, the experimental spectra were compared to the characteristic X-ray card files in the JCPDS database. Corresponding JCPDS card numbers are 98-0080 for LSGM (La_{0.9}Sr_{0.1}Ga_{0.8}Mg_{0.2}O_{2.85}), 45-0637 for LaSrGa₃O₇, 80-1806 for LaSrGaO₄, and 37-1433 for La₄Ga₂O₉.

Synthesized LSGM powders were bi-axially pressed into pellets under 70 MPa, and then isostatically pressed under 350 MPa. These pellets were heated up to 1350 °C and held 6 h at this temperature. XRD, SEM (FEG-SEM Leo Supra 35, Oberkochen, Germany) and energy dispersive X-ray spectrometry (EDS) studies were conducted on these pellets.

Amorphous LSGM (La_{0.9}Sr_{0.1}Ga_{0.85}Mg_{0.15}O_{3-δ}) films were deposited on pure gold substrates from synthesized pure LSGM pellets. The crystallization behavior of these amorphous films was studied using differential thermal analysis (Netzsch STA 449C Jupiter, Selb, Germany) and X-ray diffraction.

Complex-plane impedance measurements were performed via Solartron Impedance Analyzer 1260 with Solartron 1296 dielectric interface. Ohmic resistivities of the samples were estimated by fitting of the high-frequency arc to a semicircle and calculating the real impedance difference. The measurements were done in the frequency range of 5 Hz to 13 MHz between room temperature and 545 °C.

3. Results

X-ray diffraction analysis of the LSGM films deposited on gold substrates before and after heat treatment revealed that as-deposited films and films heat treated at 600 °C for 48 h are X-ray amorphous (Fig. 1 curve (a)). The only visible peaks in the spectrum belong to the gold substrate. Fig. 1 curve (b) illustrates the X-ray diffraction data of the same sample after heat treatment at 655 °C for 72 h. Besides the gold-diffraction peaks one can

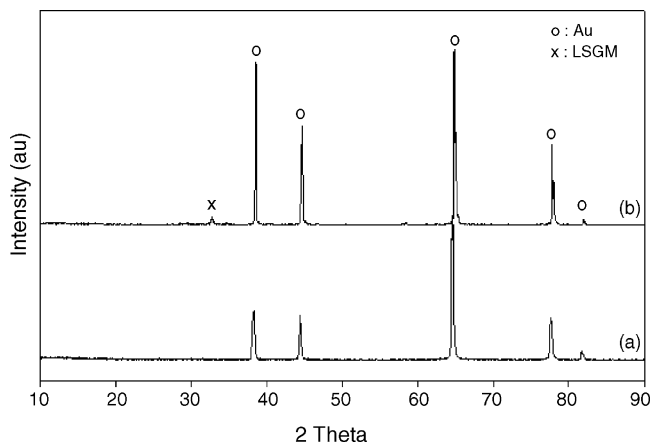


Fig. 1. XRD plot of the LSGM deposited onto 99.99% Au plate (a) annealed at 600 °C for 48 h, (b) annealed at 655 °C for 72 h.

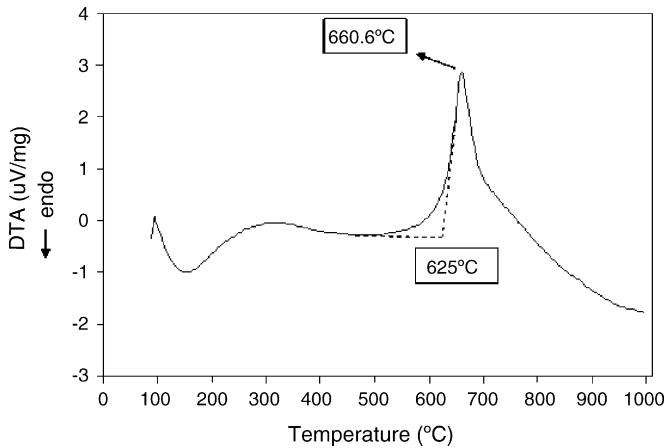


Fig. 2. DTA plot of the amorphous LSGM film deposited on a pure gold substrate.

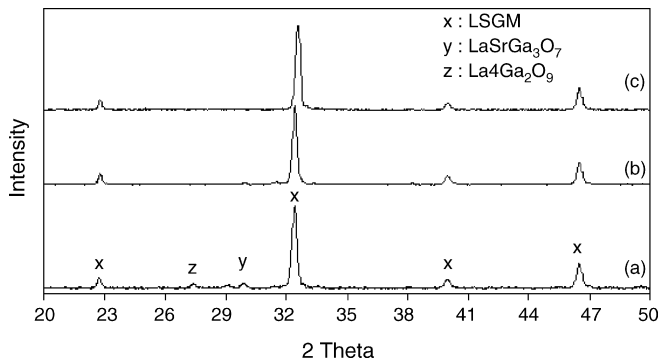


Fig. 3. XRD plot of LSGM powder with 15% Mg calcined at (a) 1150 °C, (b) 1200 °C and sintered at (c) 1350 °C for 6 h.

discern only the 100% crystalline peak of LSGM at 32.471°. Fig. 2 shows the DTA analysis results of the films on gold substrate. The exothermic peak at around 660 °C is associated with the crystallization of the LSGM film. The edge onset for the crystallization peak is at a temperature of 625 °C.

X-ray diffraction spectra from LSGM powders with 15% and 17% Mg calcined from the organic precursors at 1150 °C and 1200 °C are shown in Figs. 3 and 4 along side the spectra from the pellets sintered at 1350 °C for 6 h. Samples heat treated at

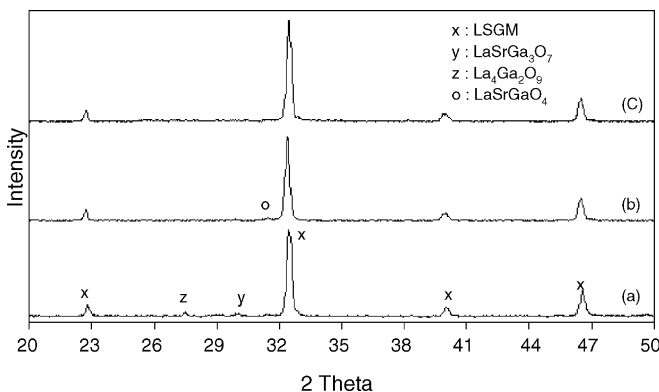
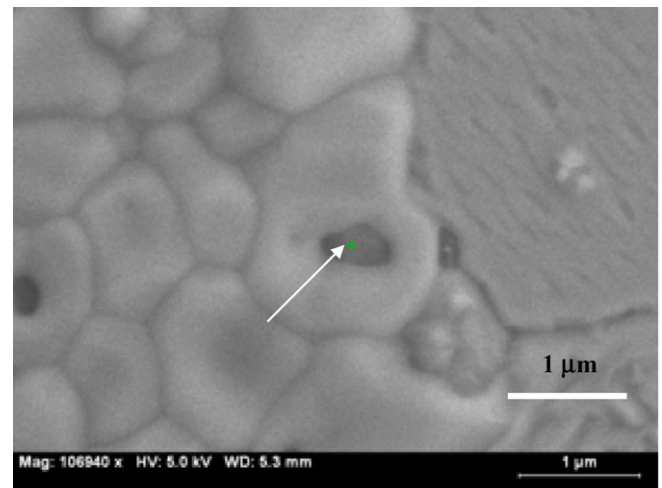


Fig. 4. XRD plot of LSGM powder with 17% Mg calcined at (a) 1150 °C, (b) 1200 °C and sintered at (c) 1350 °C for 6 h.

1150 °C and 1200 °C contained small amounts of $\text{LaSrGa}_3\text{O}_7$ (peak at 29.91°), $\text{La}_4\text{Ga}_2\text{O}_9$ (peak at 27.67°), and LaSrGaO_4 (peak at 31.40°) phases along with the main phase LSGM. With increasing temperature the amount of LSGM phase in the powders increased from 91% at 1150 °C to higher than 95% at 1200 °C.

X-ray spectra from pellets sintered from the same powders at 1350 °C for 6 h do not reveal any peaks belonging to any second phase. The material is X-ray-phase-pure LSGM.

Transmission and scanning electron microscopy analyses of the same pellets showed that MgO precipitates formed in the samples. Fig. 5a is an SEM image of the sample with 15%



(a)

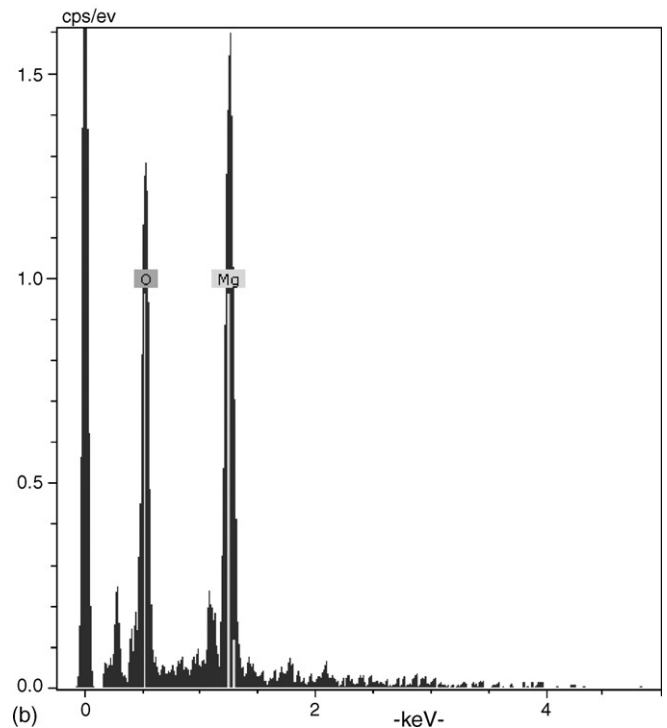


Fig. 5. (a) SEM micrograph showing several MgO particles (dark grey) in the LSGM with 15% Mg. (b) EDS analysis results of the MgO particle shown in Fig. 5a. Besides Mg and O signal one can discern a weak Ga signal at 1.1 KeV that originates in the matrix (see further discussion in the text).

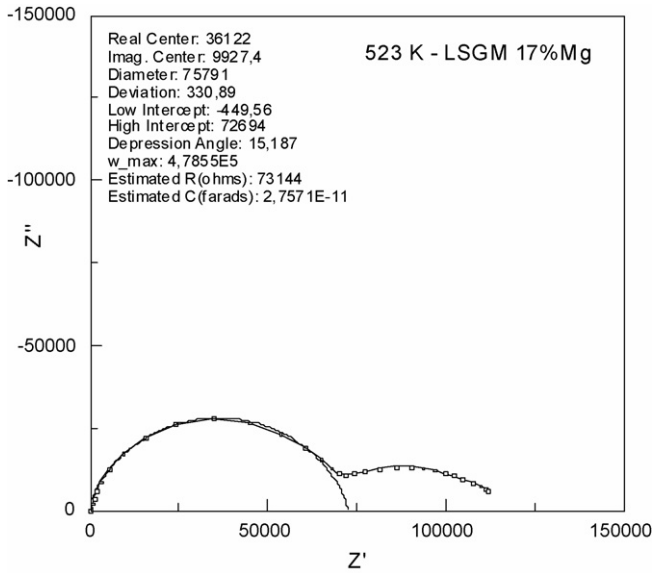


Fig. 6. Complex-plane impedance analysis data of LSGM with 10% Sr and 17% Mg where the high-frequency arc is shown with the fitted curve.

Mg in its composition. MgO precipitates (darker particles) were observed within the LSGM grains, at grain boundaries and multi-grain junctions. The MgO precipitates are fewer than 1 vol% in the microstructure and their sizes vary from 50 to 300 nm. Fig. 5b shows strong Mg and O peaks in the EDS spectrum of one of the precipitates taken with an SEM. The peak at 1.1 keV is from Ga in the matrix. Since the EDS spectra was collected with 5 keV, EDS peaks belonging to La (also from underlying matrix) were not observed.

LSGM powder compacts were sintered at 1350 °C for 6 h. The densities of the pellets measured using Archimedes method in water were in excess of 99% of the theoretical density (6.68 g/cm³). Here, the theoretical density of the LSGM was calculated according to the lattice parameters of La_{0.9}Sr_{0.1}Ga_{0.8}Mg_{0.2}O_{3-δ} composition.²¹ SEM investigation of the microstructure confirmed the densities to be in excess of 99% for both compositions that were used in this study. The sintering temperature of 1350 °C is 100 °C lower than the ones reported in the literature (1450 °C or higher).^{22–25}

Sintered pellets with $x=0.1$, $y=0.15$ and 0.17 were used in the impedance analyses at temperatures between room temperature and 545 °C. The result of complex-plane impedance measurement performed at 250 °C on sample $y=0.17$ is shown in Fig. 6. The ohmic bulk conductivity of pellets is defined as:

$$\sigma_{\text{ohm}} = \frac{1}{R_{\text{ohm}}} \times \frac{t}{A} \quad (1)$$

where R_{ohm} is ohmic resistance of the grains, t and A are the thickness and the electrode surface area of the sample, respectively. The R_{ohm} is measured from the high frequency semicircle in the complex plane impedance analysis results.

Fig. 7 is the plot of $\log(\sigma T)$ versus $1/T$ for LSGM samples with 15% and 17% Mg between room temperature and 545 °C. Data for both compositions lie on straight lines. Along with the experimental data, best linear fits to the data for the two

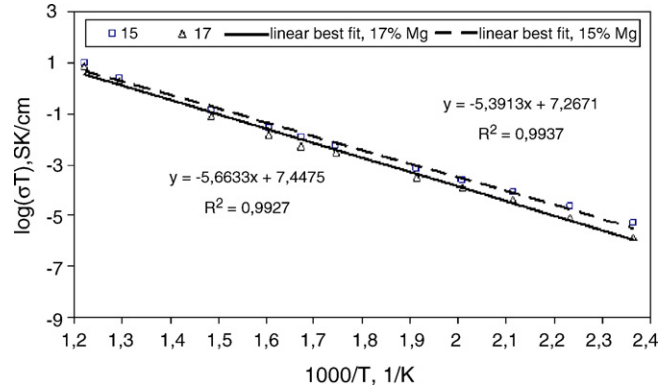


Fig. 7. Ohmic bulk conductivities as a function of temperature for two LSGM pellets with 15 at.% and 17 at.% Mg concentration. Linear best fit to the data is also superimposed on the plots.

samples are also shown. From these linear fits the ionic bulk conductivities for LSGM at 800 °C were estimated to be 0.14 and 0.16 S/cm for 17% and 15% Mg containing samples by extrapolation, respectively.

4. Discussion

The best ionic conductivity (0.17 S/cm) for the intermediate temperature (800 °C) SOFC electrolyte LSGM materials is reported for the La_{0.8}Sr_{0.2}Ga_{0.83}Mg_{0.17}O_{3-δ} composition.⁵ The reported value is better than the minimum conductivity required for a feasible operation of the fuel cell. Thus, any improvement on this value will be an added benefit. However, there is a prominent problem for the commercialization of the LSGM as an electrolyte for IT-SOFC. It is difficult to produce it as a phase pure material at a reasonably low temperature in large quantities. In this study, amorphous LSGM films were shown to start crystallizing at temperatures as low as 625 °C. Thus, it is at least in theory possible to produce single phase LSGM with the desired stoichiometry at this temperature. However, thus far it was agreed in the literature that single-phase LSGM could not be obtained easily even at 1500 °C.²⁶ Yan et al. reported that LSGM (with La_{0.9}Sr_{0.1}Ga_{0.8}Mg_{0.2}O_{3-δ} composition) powders with 99% phase purity was obtained at temperatures as low as 1120 °C.²⁷ Those powders as well as the powders produce here at 1200 °C contain few percents of LaSrGaO₄ (peak at 31.40°) phase. Using tartaric acid as the carrier material in an organic precursor method, it is now possible to produce X-ray phase pure LSGM powders at 1350 °C.

Electron microscopy (TEM and SEM coupled with EDS) studies of the samples with La_{0.9}Sr_{0.1}Ga_{0.85}Mg_{0.15}O_{3-δ} composition sintered at 1350 °C for 6 h revealed that the samples contained MgO second phase precipitates although X-ray analysis show the samples to be phase pure. Obviously, this composition of the LSGM is above the solubility limit for MgO in the mixed oxide. SEM coupled with EDS chemical analysis clearly show darker precipitates of MgO with sizes ranging from 50 nm to 300 nm. Their concentration appears to be around 1 vol.% in the microstructure. Their low concentration and small precipitate sizes may be the reason why they were not

detected in the X-ray analysis. Therefore the powders appeared to be phase pure in X-ray analysis. However, precipitation of MgO particles is indicative that the amount of Mg^{2+} ions in the bulk of the LSGM grains and at the grain boundaries reached saturation. Since MgO is a poor ionic conductor it is generally an undesired phase in the microstructure. The consolation in the observed microstructure is that the isolated particle morphology of the MgO precipitates will impose a minimum influence on the ionic conductivity of the mixed-oxide. Their effect will be limited by their volume percentage. Optimization can be obtained by determining the solubility limit of the Mg impurity in the structure. Gorelov et al. reported that the co-solubility of magnesium and strontium in lanthanum gallate matrix is about 16% for both cations.²⁸ This co-solubility condition was claimed to be valid if both cations are in equal amounts. In this study, LSGM with the following composition, $La_{0.9}Sr_{0.1}Ga_{0.85}Mg_{0.15}O_{3-\delta}$, reveal MgO precipitates confirming the previous claims by Gorelov and co-workers. Apparently, 10% Sr cannot support 15% Mg in the lanthanum gallate matrix. A change in the concentration of Sr affects the solubility of Mg. The reason for this behavior is not immediately obvious to the authors.

The impedance analysis of the samples studied here indicated the LSGM with $La_{0.9}Sr_{0.1}Ga_{1-x}Mg_xO_{3-\delta}$ (with $x=0.15$ and 0.17) compositions satisfies the minimum requirements for an IT-SOFC electrolyte. A linear relationship between $\log(\sigma T)$ and $1/T$ was determined in the temperature range investigated (RT – 545 °C). The extrapolated ionic conductivity value at 800 °C for the material would be around 0.14–0.16 S/cm. This value is on the same order of magnitude as the best reported value for LSGM. However, a simple straight-line extrapolation can be misleading. It has been reported in the literature that the slope of the $\log(\sigma T)$ versus $1/T$ plot changes above 550 °C.²⁹ Further studies of the ionic conductivity at higher temperatures are absolutely required. Another important aspect in Fig. 7 is that the data for the two compositions lie on straight lines with different slopes. This could be indicative that the solubility limit -and with it, the benefit of adding the dopant to create additional oxygen vacancies in the matrix-may be strongly temperature-dependent in this temperature range. The solubility of the two dopants, i.e., Sr and Mg has to be investigated as a function of temperature. The change in the slope of the $\log(\sigma T)$ versus $1000/T$ which is claimed in the literature may be related to a change in the solubility of the dopants. Along with the observed morphology of the MgO precipitates in the LSGM microstructure, the impedance measurements of the two samples confirm that the negative influence of MgO precipitates on ionic conductivity is limited at these concentrations.

5. Conclusions

Crystallization temperature of an amorphous LSGM film was determined as ~625 °C. This is most likely the theoretical lower temperature limit for the single phase LSGM synthesis. X-ray single-phase LSGM pellets with $La_{0.9}Sr_{0.1}Ga_{1-x}Mg_xO_{3-\delta}$ (with $x=0.15$ and 0.17) compositions were synthesized via organic precursor method using tartaric acid as the organic car-

rier, at 1350 °C. Dense and X-ray single-phase LSGM pellets (>99% theoretical density) were sintered at the same temperature by holding the powder compacts for 6 h. These lower synthesis and sintering temperatures eliminate problems associated with the gallium loss at temperatures in excess of 1400 °C.

Bulk ionic conductivities of the samples were measured by impedance analysis between room temperature and 545 °C. The extrapolated ionic conductivity could be as high as 0.14–0.16 S/cm at 800 °C. This value is very promising, however, caution should be exercised in interpreting this extrapolated ionic conductivity value. A change in the slope of $\log(\sigma T)$ versus $1/T$ plot is suspected in the literature above 550 °C.

Electron microscopy analysis revealed that the reported composition is above the solubility limit for Mg in the material at room temperature. However, there are indications that Mg solubility may change with respect to temperature. MgO precipitates (50–300 nm) were observed in the microstructure with the help of TEM and SEM analysis. It may be possible to further improve the ionic conductivity of the material by optimizing the composition.

Acknowledgements

This work was supported by TUBITAK MISAG-244 Project. The authors thank to Prof. C.B. Carter and Arzu Altay both at University of Minnesota for their help with the PLD and TEM experiments and many fruitful discussions, to Prof. Osman Gurdal, Prof. Muzaffer Balbasi, Prof. Metin Guru and Ahmet Kayis from Gazi University – GIMBAM Laboratories, for their help with the impedance analysis studies via the DPT project no: 2001K120590.

References

1. Oncel, C. and Gulgun, M. A., Synthesis of $LaSrXMg$ -oxide with $X = Ga, Fe,$ or Cr . In *Proceedings of the Materials Research Society, Vol 756*. Materials Research Society, Pittsburgh, PA, 2003, pp. 497–502.
2. Tas, A. C., Majewski, P. J. and Aldinger, F., Chemical preparation of pure strontium- and/or magnesium-doped lanthanum gallate powders. *Journal of the American Ceramic Society*, 2000, **83**, 2954–2960.
3. Fleig, J., Kreuer, K. D. and Maier, J., *Handbook of Advanced Ceramics. Materials, Applications, and Processing*. Academic Press, 2001, pp. 1–60.
4. Ullmann, H. and Trofimenko, N., Optimisation of composite cathodes for intermediate temperature SOFC applications. *Solid State Ionics*, 1999, **126**, 163–174.
5. Huang, K., Tichy, R. S. and Goodenough, J. B., Superior perovskite oxide-ion conductor; strontium- and magnesium-doped $LaGaO_3$: I, phase relationships and electrical properties. *Journal of the American Ceramic Society*, 1998, **81**, 2565–2575.
6. Oncel, C., Chemical synthesis of multi-cation oxide powders for solid oxide fuel cell (SOFC) components. MSc Thesis, Sabanci University, Istanbul, 2003.
7. Polini, R., Falsetti, A. and Traversa, E., Sol-gel synthesis and characterization of Co-doped LSGM perovskites. *Journal of the European Ceramic Society*, 2005, **25**, 2593–2598.
8. Huang, K. and Goodenough, J. B., A solid oxide fuel cell based on Sr- and Mg-doped $LaGaO_3$ electrolyte: the role of a rare-earth oxide buffer. *Journal of Alloys and Compounds*, 2000, **303–304**, 454–464.
9. Huang, K., Tichy, R. and Goodenough, J. B., Superior perovskite oxide-ion conductor; strontium- and magnesium-doped $LaGaO_3$: III, performance

- tests of single ceramic fuel cells. *Journal of the American Ceramic Society*, 1998, **81**, 2581–2585.
10. Yi, J. Y. and Choi, G. M., Phase characterization and electrical conductivity of $\text{LaSr}(\text{GaMg})_{1-x}\text{Mn}_x\text{O}_3$ system. *Solid State Ionics*, 2002, **148**, 557–565.
 11. Eror, N. G. and Anderson, H. U., Polymeric synthesis of ceramic materials. In *Proceedings of the Materials Research Society, Vol. 73*. Materials Research Society, Pittsburgh, PA, 1986, pp. 571–577.
 12. Uchiyama, O., Kakihana, M., Arima, M., Yashima, M., Suzuki, Y. and Yoshimura, M., Polymerized complex precursors for the synthesis of high pure PbTiO_3 powders at 400–600 °C. In N. Mizutani et al. ed., *Proceedings of the Advanced Materials '93, I/A: Ceramics, Powders, Corrosion and Advanced Processing*, Transactions Material Research Society Japan, Vol. 14A, pp. 743–746.
 13. Mathews, T., Manoravi, P., Antony, M. P., Sellar, J. R. and Muddle, B. C., Fabrication of $\text{La}_{1-x}\text{Sr}_x\text{Ga}_{1-y}\text{Mg}_y\text{O}_{3-(x+y)/2}$ thin films by pulsed laser ablation. *Solid State Ionics*, 2000, **135**, 397–402.
 14. Shkerin, S. N., Bronin, D. I., Kovyazina, S. A., Gorelov, V. P., Kuzmin, A. V., Martemyanova, Z. S. et al., Structure and phase transitions of $(\text{La, Sr})(\text{Ga, Mg})\text{O}_{3-\delta}$ solid electrolyte. *Solid State Ionics*, 2004, **171**, 129–134.
 15. Gomes, E., Soares, M. R., Figueiredo, F. M. and Marques, F. M. B., Conductivity of $\text{La}_{0.95}\text{Sr}_{0.05}\text{Ga}_{0.90}\text{Mg}_{0.10}\text{O}_{3-\delta}$ obtained by mechanical activation. *Journal of the European Ceramic Society*, 2005, **25**, 2599–2602.
 16. Yamaji, K., Nigeshi, H., Horita, T., Sakai, N. and Yokokawa, H., Vaporization process of Ga from doped LaGaO_3 electrolytes in reducing atmospheres. *Solid State Ionics*, 2000, **135**, 389–396.
 17. Stevenson, J. W., Armstrong, T. R., Pederson, L. R., Li, J., Lewinsohn, C. A. and Baskaran, S., Effect of A-site cation nonstoichiometry on the properties of doped lanthanum gallate. *Solid State Ionics*, 1998, **113–115**, 571–583.
 18. Badwal, S. P. S., Stability of solid oxide fuel cell components. *Solid State Ionics*, 2001, **143**, 39–46.
 19. Oncel, C. and Gulgun, M. A. LSGM electrolyte synthesis for SOFC via an organic precursor method. in preparation.
 20. Oncel, C. and Gulgun, M. A., Chemical synthesis of LSGM powders for solid oxide fuel cell (SOFC) electrolyte. *Ceramic Transactions*, 2005, **161**, 61–68.
 21. Slater, P. R., Irvine, J. T. S., Ishihara, T. and Takita, Y., The structure of the oxide ion conductor $\text{La}_{0.9}\text{Sr}_{0.1}\text{Ga}_{0.8}\text{Mg}_{0.2}\text{O}_{2.85}$ by powder neutron diffraction. *Solid State Ionics*, 1998, **107**, 319–323.
 22. Subasri, R., Mathews, T. and Sreedharan, O. M., Microwave assisted synthesis and sintering of $\text{La}_{0.9}\text{Sr}_{0.1}\text{Ga}_{0.83}\text{Mg}_{0.17}\text{O}_{2.815}$. *Materials Letters*, 2003, **57**, 1792–1797.
 23. Polini, R., Pamio, A. and Traversa, E., Effect of synthetic route on sintering behaviour, phase purity and conductivity of Sr- and Mg-doped LaGaO_3 perovskites. *Journal of the European Ceramic Society*, 2004, **24**, 1365–1370.
 24. Gomes, E., Soares, M. R., Figueiredo, F. M. and Marques, F. M. B., Conductivity of $\text{La}_{0.95}\text{Sr}_{0.05}\text{Ga}_{0.9}\text{Mg}_{0.1}\text{O}_{3-\delta}$ obtained by mechanical activation. *Journal of the European Ceramic Society*, 2005, **25**, 2599–2602.
 25. Polini, R., Falsetti, A. and Traversa, E., Sol-gel synthesis and characterization of Co-doped LSGM perovskites. *Journal of the European Ceramic Society*, 2005, **25**, 2593–2598.
 26. Liu, N., Shi, M., Yuan, Y. P., Chao, S., Feng, J. P., Majewski, P. et al., Thermal shock and thermal fatigue study of Sr- and Mg-doped lanthanum gallate. *International Journal of Fatigue*, 2006, **28**, 237–242.
 27. Yan, J., Dong, Y., Yu, C. and Jiang, Y., Synthesis of $\text{La}_{0.9}\text{Sr}_{0.1}\text{Ga}_{0.8}\text{Mg}_{0.2}\text{O}_{3-\delta}$ by improved citric acid routine and characterization of its properties of electrical conductivities. Solid oxide fuel cells VII. *Symposium, Electrochemical Society Proceedings, Vol 16*, 2001, pp. 358–367.
 28. Gorelov, V. P., Bronin, D. I., Sokolova, Ju. V., Nafe, H. and Aldinger, F., The effect of doping and processing conditions on properties of $\text{La}_{1-x}\text{Sr}_x\text{Ga}_{1-y}\text{Mg}_y\text{O}_{3-\alpha}$. *Journal of the European Ceramic Society*, 2001, **21**, 2311–2317.
 29. Pelosato, R., Sora, I. N., Ferrari, V., Dotelli, G. and Mari, C. M., Preparation and characterisation of supported $\text{La}_{0.83}\text{Sr}_{0.17}\text{Ga}_{0.83}\text{Mg}_{0.17}\text{O}_{2.83}$ thick films for application in IT-SOFCs. *Solid State Ionics*, 2004, **175**, 87–92.